On the interaction of the responses at the resonance frequencies of a nonlinear two degrees-of-freedom system

Gianluca Gatti, Michael J. Brennan, Ivana Kovacic

On the interaction of the responses at the resonance frequencies of a nonlinear two degrees-of-freedom system

Gianluca Gatti [a], Michael J. Brennan [b], Ivana Kovacic [c]

[a] Department of Mechanical Engineering, University of Calabria, Arcavacata di Rende (CS), 87036, Italy
[b] Institute of Sound and Vibration Research, University of Southampton, Southampton, SO17 1BJ, United Kingdom
[c] Faculty of Technical Sciences, Department of Mechanics, University of Novi Sad, Novi Sad, 21125, Serbia

This paper describes the dynamic behaviour of a coupled system which includes a nonlinear hardening system driven harmonically by a shaker. The shaker is modelled as a linear single degree-of-freedom system and the nonlinear system under test is modelled as a hardening Duffing oscillator. The mass of the nonlinear system is much less than the moving mass of the shaker and thus the nonlinear system has little effect on the shaker dynamics. The nonlinearity is due to the geometric configuration consisting of a mass suspended on four springs, which incline as they are extended. Following experimental validation, the model is used to explore the dynamic behaviour of the system under a range of different conditions. Of particular interest is the situation when the linear natural frequency of the nonlinear system is less than the natural frequency of the shaker such that the frequency response curve of the nonlinear system bends to higher frequencies and thus interacts with the resonance frequency of the shaker. It is found that for some values of the system parameters a complicated frequency response curve for the nonlinear system can occur; closed detached curves can appear as a part of the overall amplitude-frequency response. These detached curves can lie outside or inside the main resonance curve, and a physical explanation for their occurrence is given.

1. Introduction

The behaviour of forced nonlinear two degrees-of-freedom (dof) coupled oscillators has been reported extensively in the literature, mainly by researchers investigating the dynamics of vibration absorbers.

Shaw et al. [1] considered a coupled system where the main and auxiliary springs are with a linear-plus-cubic term. By applying the method of multiple scales, they found that when the excitation frequency is halfway between their resonances, coexisting trivial and quasi-periodic steady-state solutions occur, implying that the presence of the nonlinearities can result in an amplification rather than a reduction of the vibration amplitudes. Studying a system with nonlinear damping and nonlinear springs, Zhu et al. [2] showed that a reduction of the vibration amplitude can be obtained by properly selecting the parameters of the nonlinear dampers, nonlinear spring stiffness and excitation frequency. Resonant interactions between coupled linear and nonlinear components have been identified as the primary phenomena behind "energy pumping" (see, for example, [3–8]). In [3], it was investigated theoretically how the system comprising a forced linear oscillator and a strongly purely cubic attachment behaves in the vicinity of a main resonance. A possible quasi-periodic response was discovered and its advantages from the viewpoint of vibration suppression were confirmed experimentally. These quasi-periodic vibrations have also been found experimentally by testing a small building, but their occurrence was detected for a certain range of the excitation amplitudes only [4]. In the first paper in a series of two, Gendelman et al. [5] studied various coexisting response regimes of this system, computed their domains of existence and analysed other characteristics, such as breakdown of the resonance, phase locking, etc. A possible application of this system for vibration mitigation and absorption was described in the second paper [6]. Further considering the same system [7], the authors illustrated the local bifurcations of the periodic solutions via frequency-response curves (FRCs), showing their evolution with the increase of the excitation amplitude. As a distinguishable feature, a closed detached resonance curve, which occurs above the main resonance curve, was depicted. With the increase of

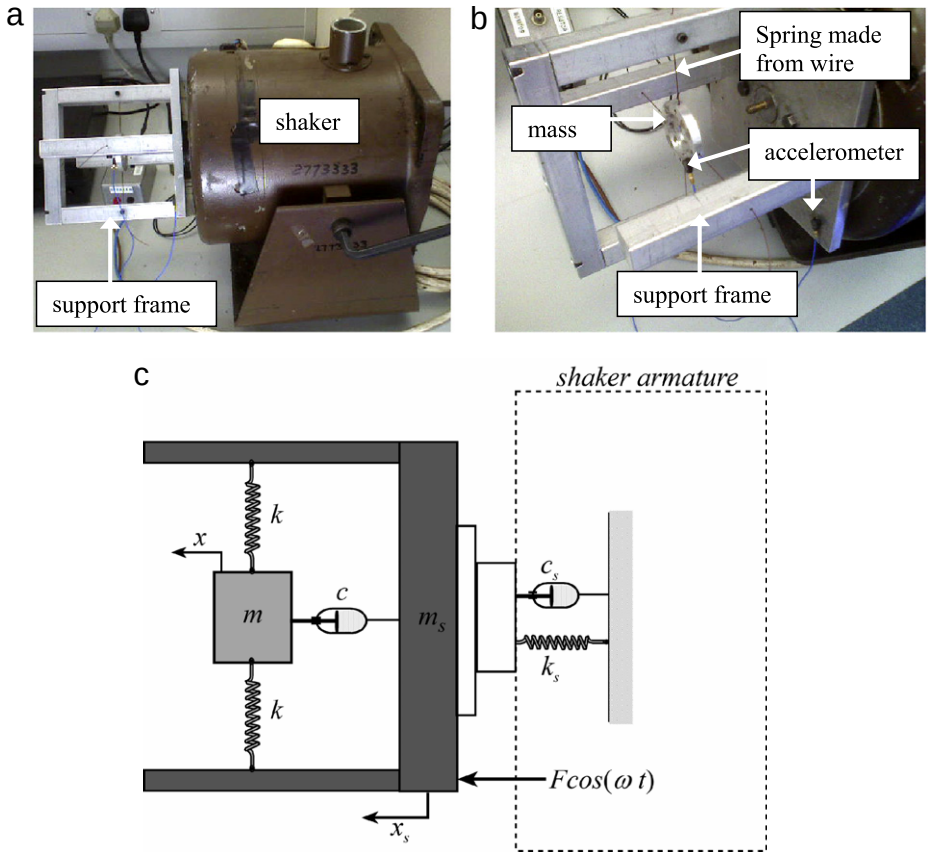

Fig. 1. Practical system under consideration, consisting of a nonlinear system attached to an electro-dynamic shaker. (a) Photograph of the system, (b) Photograph showing the details of the nonlinear system attached to the shaker, (c) Schematic view.

the excitation amplitude, it approaches the main resonance curve, merges with it and a new shape of a continuous FRC with a peak is formed. The coexistence of three distinct regimes, two of which are periodic and the third one being quasi-periodic, was also presented. In [8], the co-existence of two types of the steady state solution, one of which belongs to a detached part was also shown theoretically and confirmed experimentally. It was demonstrated in [9], that if this system has a piecewise-quadratic damping characteristic and is properly tuned, dangerous periodic regimes arising due to this detached curve can be completely annihilated. In a recent paper, Alexander and Schilder [10] identified numerically the presence of a detached resonance curve for a system with a cubic term but with a negligible linear term.

In this paper we analyse an experimental set-up in which an electro-dynamic shaker is used to excite a geometrically nonlinear attachment which has a much smaller mass than the shaker. The system is modelled as a nonlinear hardening Duffing oscillator coupled to a linear system, representing the shaker. In the analysis of the corresponding dynamic behaviour, of particular interest is the situation where the linear resonance frequency of the nonlinear system under test is lower than the resonance frequency of the shaker. Because the system is hardening, the frequency response curve of the nonlinear system bends to higher frequencies and thus interacts with the resonance frequency of the shaker. Investigating analytically and numerically the effects of the system parameters on its response, coexisting steady states are found, with some detached resonance curves appearing in the FRCs. These detached resonance curves can lie above or inside the main resonance curve. The latter is named after its shape, a "bubble". As far as the authors are aware, such a detached resonance curve has not been identified yet as a part of the amplitude-frequency response.

2. Nonlinear system excited by an electro-dynamic shaker

2.1. System description

The practical system of interest in this paper is depicted in Fig. 1. Photographs are shown in Fig. 1(a) and (b), and a schematic representation is shown in Fig. 1(c). A small mass m, is attached to a large shaker via a support frame. The four springs between the small mass and the support frame are made from fishing line, which can be modelled as a stiffness k and a damper c. The initial tension in the wires can be adjusted and has a profound effect on the stiffness of the system attached to the shaker. When the small mass vibrates in the horizontal direction, the springs stretch in tension, thus creating a geometric nonlinearity. The electro-dynamic shaker, which is used to excite the system, can be modelled as a linear system consisting of a parallel combination of a spring k_s and a damper c_s connected to a mass m_s, which is made up of the moving mass of the shaker and the support frame, and is much larger than the mass m. If the shaker is driven with a constant current at each frequency, the excitation can be modelled as a harmonic force with constant amplitude, $F\cos(\omega t)$ as shown in Fig. 1(c).

2.2. System modeling

The wires connecting the small mass to the support structure can be modelled as shown in Fig. 2(a). The distance d, is equal to the length of the spring when the system is at rest. When the mass moves in the z direction, the springs incline to accommodate the motion as shown in the figure and it is this change in their length that is the cause of the nonlinearity. The relationship between

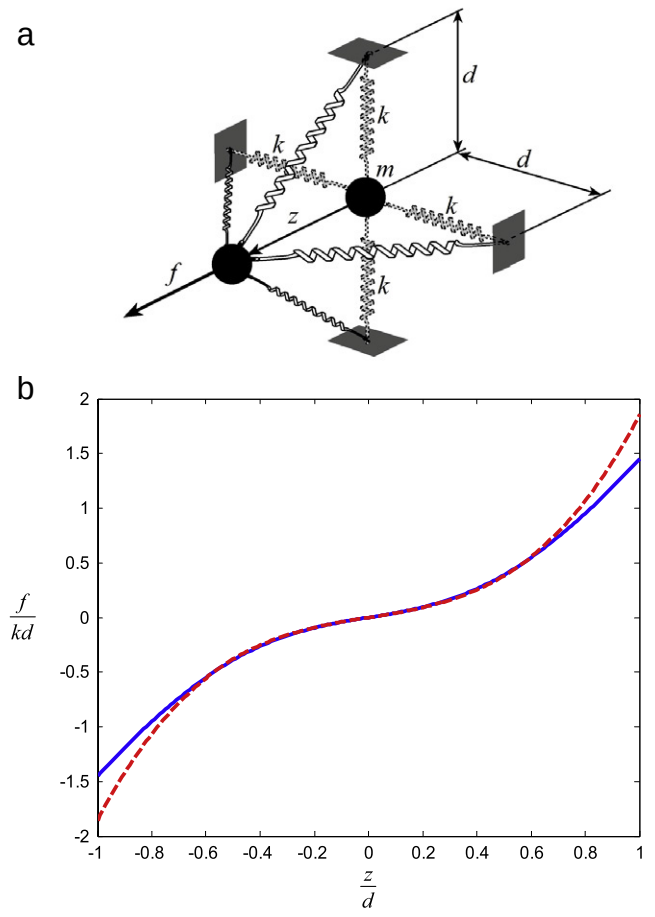

Fig. 2. The nonlinear system attached to the shaker. (a) Schematic view, (b) Non-dimensional reaction force as a function of the non-dimensional relative displacement of the mass for $d_o/d = 0.9$; exact expression given by Eq. (1) (blue solid line), approximate expression defined by Eq. (2) (red dashed line).

the applied static force f in Fig. 2(a), and the resulting relative displacement z is given by

$$f = 4kz\left(1 - \frac{d_0}{\sqrt{z^2 + d^2}}\right), \tag{1}$$

where $d_0 \leq d$ is the length of the unstretched spring. Using the Taylor-series expansion to the third order for small z, Eq. (1) can be written as

$$f \approx k_1 z + k_3 z^3, \tag{2}$$

where $k_1 = 4k\left(1 - \frac{d_0}{d}\right)$ and $k_3 = 2k\frac{d_0}{d^3}$. The non-dimensional form of Eq. (1) and its approximation given by Eq. (2) are illustrated in Fig. 2(b), for the particular case when $\frac{d_0}{d} = 0.9$. It can be seen that for a relative displacement z, less than 40% of the length d, the percentage error between Eqs. (1) and (2) is less than 5%. Furthermore, this error decreases for decreasing values of $\frac{d_0}{d}$.

Using the approximate expression for the spring restoring force, the equations of motion of the two dof system depicted in Fig. 1(c) are

$$m_s\ddot{x}_s + c_s\dot{x}_s + k_s x_s + c\left(\dot{x}_s - \dot{x}\right) + k_1\left(x_s - x\right) + k_3\left(x_s - x\right)^3 = F\cos\left(\omega t\right) \tag{3a}$$

$$m\ddot{x} - c\left(\dot{x}_s - \dot{x}\right) - k_1\left(x_s - x\right) - k_3\left(x_s - x\right)^3 = 0, \tag{3b}$$

which correspond to the simplified system depicted in Fig. 3. Eqs. (3a) and (3b) can be written in non-dimensional form as

$$\left(w'' + y''\right) + 2\zeta_s\left(w' + y'\right) + \left(w + y\right)$$

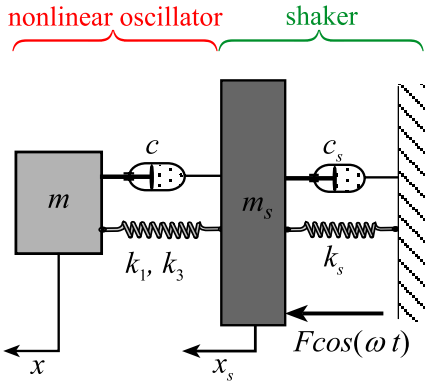

Fig. 3. Simplified model of the nonlinear system attached to the shaker.

$$+ 2\mu\zeta w' + \mu\omega_0^2 w + \mu\gamma w^3 = \cos\left(\Omega\tau\right) \tag{4a}$$

$$y'' - 2\zeta w' - \omega_0^2 w - \gamma w^3 = 0, \tag{4b}$$

where $z = x_s - x$, $(\cdot)' = \mathrm{d}(\cdot)/\mathrm{d}\tau$, and the following non-dimensional variables are introduced

$$y_s = \frac{x_s}{x_0}, \quad y = \frac{x}{x_0}, \quad w = \frac{z}{x_0}, \quad x_0 = F/k_s,$$

$$\omega_s = \sqrt{k_s/m_s}, \quad \omega_1 = \sqrt{k_1/m}, \quad \tau = \omega_s t, \quad \Omega = \frac{\omega}{\omega_s},$$

$$\mu = \frac{m}{m_s}, \quad \gamma = \frac{k_3}{\mu k_s}x_0^2, \quad \zeta_s = \frac{c_s}{2m_s\omega_s},$$

$$\zeta = \frac{c}{2m\omega_s}, \quad \omega_0 = \frac{\omega_1}{\omega_s}.$$

It should be noted that a change in γ can be interpreted as a change in the nonlinearity or in the amplitude of excitation or in the mass ratio. It is also noted that x_0, as defined above, represents the static displacement of the system at $\omega = 0$. Assuming that $\left|\mu y''\right| \ll \left|y_s''\right|$, as in the practical situation discussed in this paper, Eqs. (4a) and (4b) can be written as

$$y_s'' + 2\zeta_s y_s' + y_s = \cos\left(\Omega\tau\right) \tag{5a}$$

$$w'' + 2\zeta w' + \omega_0^2 w + \gamma w^3 = y_s''. \tag{5b}$$

Eq. (5a) shows that the nonlinear system attached to the shaker has a negligible effect on the shaker vibration so that the shaker vibrates predominantly as a linear system, while Eq. (5b) describes a base-excited hardening Duffing oscillator. Approximate solutions for the equations of motion given by Eqs. (5a) and (5b) are found by the harmonic balance method (HBM), where the responses are assumed to be at the frequency of excitation and are given by

$$y_s = Y_s\cos\left(\Omega\tau + \varphi_s\right) \tag{6a}$$

$$w = W\cos\left(\Omega\tau + \varphi\right). \tag{6b}$$

Substituting Eqs. (6a) and (6b) into Eqs. (5a) and (5b) and applying the HBM results in

$$Y_s^2\left[\left(1 - \Omega^2\right)^2 + 4\zeta_s^2\Omega^2\right] = 1 \tag{7a}$$

$$\frac{9}{16}\gamma^2 W^6 + \frac{3}{2}\gamma W^4\left(\omega_0^2 - \Omega^2\right) + W^2\left(\Omega^4 + 4\zeta^2\Omega^2 + \omega_0^4 - 2\omega_0^2\Omega^2\right) - \Omega^4 Y_s^2 = 0. \tag{7b}$$

Eqs. (7a) and (7b) form a set algebraic equations in which Eq. (7a), which describes the frequency response of the shaker, is decoupled from Eq. (7b). However Eq. (7b) is coupled with Eq. (7a) by the amplitude of the response of the shaker Y_s. Note that Eq. (7b) is cubic in W^2. The same expressions as those in Eqs. (7a) and (7b) were also found by using the method of multiple scales. The

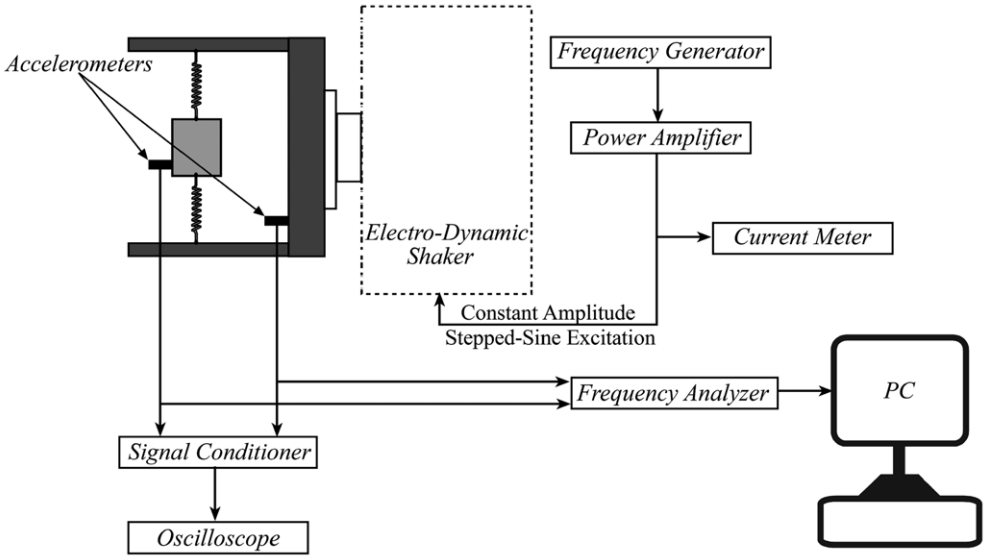

Fig. 4. Experimental setup.

stability of the solutions were calculated following the procedure in [11,12] and the limits for stability were determined to be

$$\Omega_{1,2} = \left(\left(\frac{3}{2}W^2\gamma - 2\zeta^2 + \omega_0^2\right) \pm \left(\left(-\frac{3}{2}W^2\gamma + 2\zeta^2 - \omega_0^2\right)^2 - \frac{27}{16}W^4\gamma^2 - \omega_0^4 - 3W^2\gamma\omega_0^2\right)^{\frac{1}{2}}\right)^{\frac{1}{2}}. \quad (8a, b)$$

The stable solutions are shown as solid lines and unstable solutions as dashed lines in the simulated FRCs shown in Figs. 6–8. Before these can be plotted, however, experimental work is required to determine some of the system parameters so that the predictions from the model can be compared with the experimental results.

2.3. Experimental work

The experimental setup is depicted in Fig. 4. The electro-dynamic shaker was driven by a signal generator supplying a stepped-sine signal. Accelerometers (PCB type 352C22) were attached to the support structure and to the small mass as shown in Fig. 4, while a signal conditioner (PCB model 442C04) and a two-channel oscilloscope were used to observe the system response.

Before collecting data, two tests were carried out to broadly investigate the dynamic behaviour of the system. For each test, the support wires had a different initial tension. In the first test, a slow frequency sweep (where the shaker was driven by a constant voltage) was applied from zero to about 28 Hz and the response of the system was monitored using the oscilloscope. The first resonance was observed at about 19 Hz, with both masses vibrating with large amplitudes. As the frequency was increased beyond this, a second resonance occurred at about 26 Hz, in which only the vibration of the suspended mass was large. This was followed by a sudden decrease in the motion of the suspended mass (a jump-down), which can be seen in the attached movie movie 1. The frequency was then slowly swept down. A sudden increase in the amplitude was observed at a frequency of about 22 Hz, again for the suspended mass only (a jump-up), which can be seen in the attached movie movie 2. At about 19 Hz, the resonance response in which there was large motion of both the support structure and the suspended mass was observable. In the second test similar behaviour was observed, but the jump-up and jump-down frequencies were found to occur at about 29 Hz and 34 Hz respectively.

To collect data, the shaker was then driven at discrete frequencies for the system with the wires set with low and high initial tensions, corresponding to the cases described above, respectively. The excitation frequency was increased from 10 Hz to 36 Hz, with 1 Hz increments, and then decreased to 10 Hz with the same frequency increments. As mentioned previously, the amplitude of the excitation force was maintained at a constant level for all excitation frequencies, by manually adjusting the power amplifier so that the current was 0.8 A. At each frequency, once the system was in a steady-state, five-second acceleration time histories were captured using a DataPhysics frequency analyser connected to a PC. Subsequently, these data were processed to give the displacement of the support structure and the suspended mass. The data are presented in terms of the absolute displacement x_s of the support structure and the relative displacement $z = x_s - x$ between the support structure and the suspended mass. The Fourier's series coefficients were extracted from these two time histories and the amplitude of the first harmonic of each data set is plotted at the corresponding frequency. This can be seen in Fig. 5(a) and (b) for the system in which the springs have a low initial tension, and in Fig. 5(c) and (d) for the high initial tension springs, respectively. The data points in each graph are denoted by '+' for increasing frequency and '×' for decreasing frequency.

In Fig. 5(a) and (c), which depict the response of the support structure, it can be seen that, in each case, the FRC is similar, resembling the response of a single-degree-of-freedom linear system. The peak, at about 19.5 Hz corresponds broadly to the resonance frequency of the shaker and the attached mass of the support structure. It is evident, therefore, that the nonlinear system attached to the shaker has only a small effect on its response. This is because the combined mass of the moving part of the shaker and support structure is much greater than that of the suspended mass.

In the FRCs of the relative displacement Z, depicted in Fig. 5(b) and (d), in addition to the peak associated with the resonance frequency of the shaker, a jump-down and a jump-up frequency can be seen. These are due to the response of the suspended mass. The jump-down frequencies occur at approximately 26 Hz and 33 Hz for the low initial tension and high initial tension cases, respectively, and the corresponding jump-up frequencies at about 21 Hz and 31 Hz.

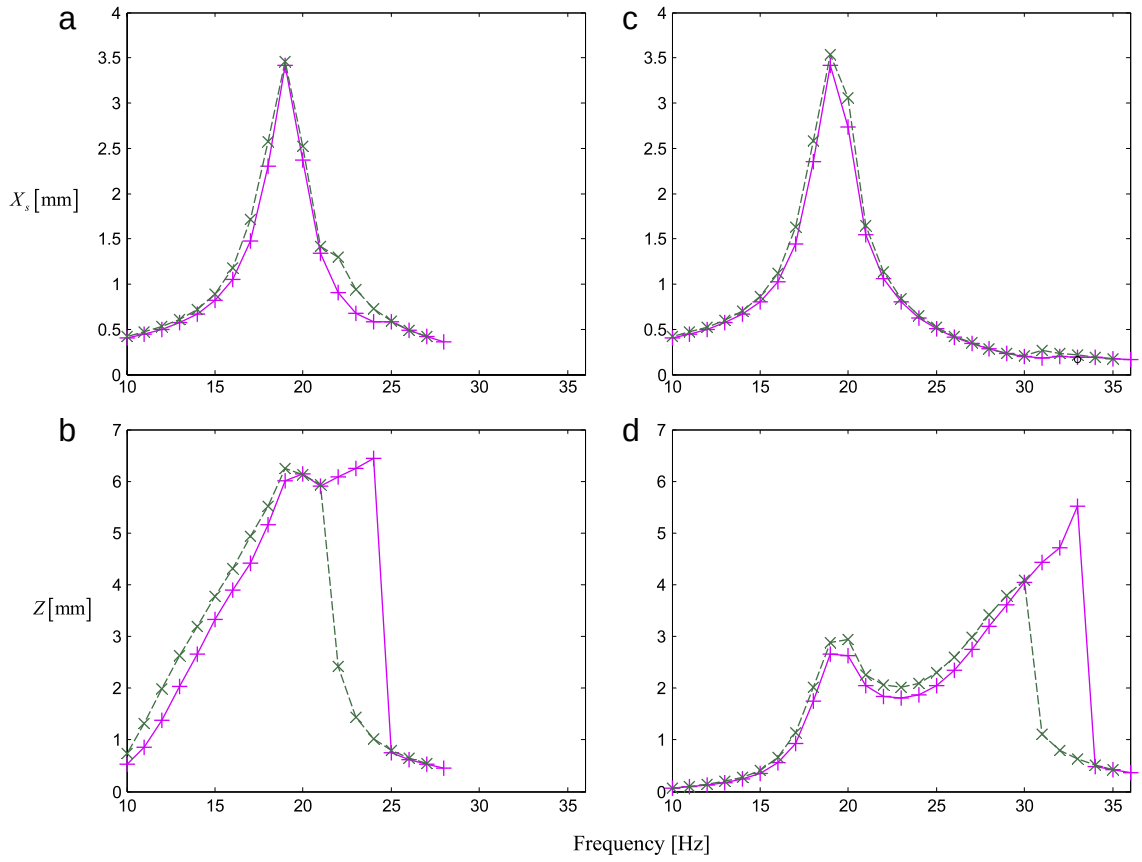

Fig. 5. Experimental results for a stepped-sine input to the shaker with a constant force amplitude. Wires with a low initial tension: (a) Absolute displacement of the support structure, (b) Relative displacement between the suspended mass and support structure. Wires with a high initial tension: (c) Absolute displacement of the support structure, (d) Relative displacement between the suspended mass and support structure. Increasing frequency (magenta '+'), decreasing frequency (green '×').

Table 1
The system parameters in Eqs. (3a) and (3b) for the two different experimental tests.

	m_s (kg)	c_s (N s/m)	k_s (N/m)	m (kg)	c (N s/m)	k_1 (N/m)	k_3 (N/m^3)	F (N)
Wires with low initial tension	1.72	19.12	2.51×10^4	19.4×10^{-3}	(0.234)	(1.3×10^2)	(1.1×10^7)	8.59
Wires with high initial tension	1.72	19.12	2.51×10^4	19.4×10^{-3}	(0.122)	(5.5×10^2)	(1.3×10^7)	8.59

Numerical values in parentheses are estimated by fitting the FRC to the experimental data.

Table 2
Equivalent non-dimensional system parameters in Eqs. (4a) and (4b).

	μ	ω_0	γ	ζ_s	ζ
Wires with low initial tension	0.011	0.677	4.6×10^{-3}	0.046	0.050
Wires with high initial tension	0.011	1.394	5.4×10^{-3}	0.046	0.026

2.4. Parameter estimation and model validation

To compare the experimental results with the predictions from the model, the system parameters were required. One group of parameters (m_s, k_s, c_s, m) was measured independently, and the other group (k_1, k_3, c) was considered to be unknown and chosen so that the FRCs were a best fit to the experimental data. The first group was estimated as follows. The combined mass of the moving part of the shaker and the support structure m_s, together with the stiffness k_s and damping c_s of the shaker were estimated through measurements made from an impact hammer test. With the suspended mass m detached and measured directly, the Frequency Response Function (FRF) of the shaker and attached support structure was measured. The system parameters were estimated by fitting a theoretical single dof FRF to the experimental FRF. Once these parameters were estimated, the electro-mechanical constant of the shaker, defined as the ratio of the force over the electric current (assumed to be constant), could be estimated by measuring the FRF of the same system when driven by a random signal from the DataPhysics signal generator through the power amplifier. For a given input current of 0.8 A, the force amplitude was then calculated and is given in Table 1.

The second group of parameters was then chosen to best fit the experimental data as follows. Noting that, for fairly weak nonlinearity, the damping has a negligibly small affect on the jump-up frequency and the corresponding FRC amplitude [13], a first two-parameter fit was performed to match those values and k_1, k_3 were estimated. The remaining parameter c was then estimated by fitting the jump-down frequency value, which is affected by the degree of nonlinearity and damping. These three parameters are also listed in Table 1, but in parentheses to indicate that they were estimated this way. For completeness, Table 2 lists the equivalent system parameters for the equation of motion written in the non-dimensional form of Eqs. (4a) and (4b).

Using the parameters in Table 2 and their relation to the dimensional parameters in Table 1, the frequency response curves described by Eqs. (7a) and (7b) are plotted in Fig. 6 (a)–(d) together with the experimental results for comparison. The FRCs

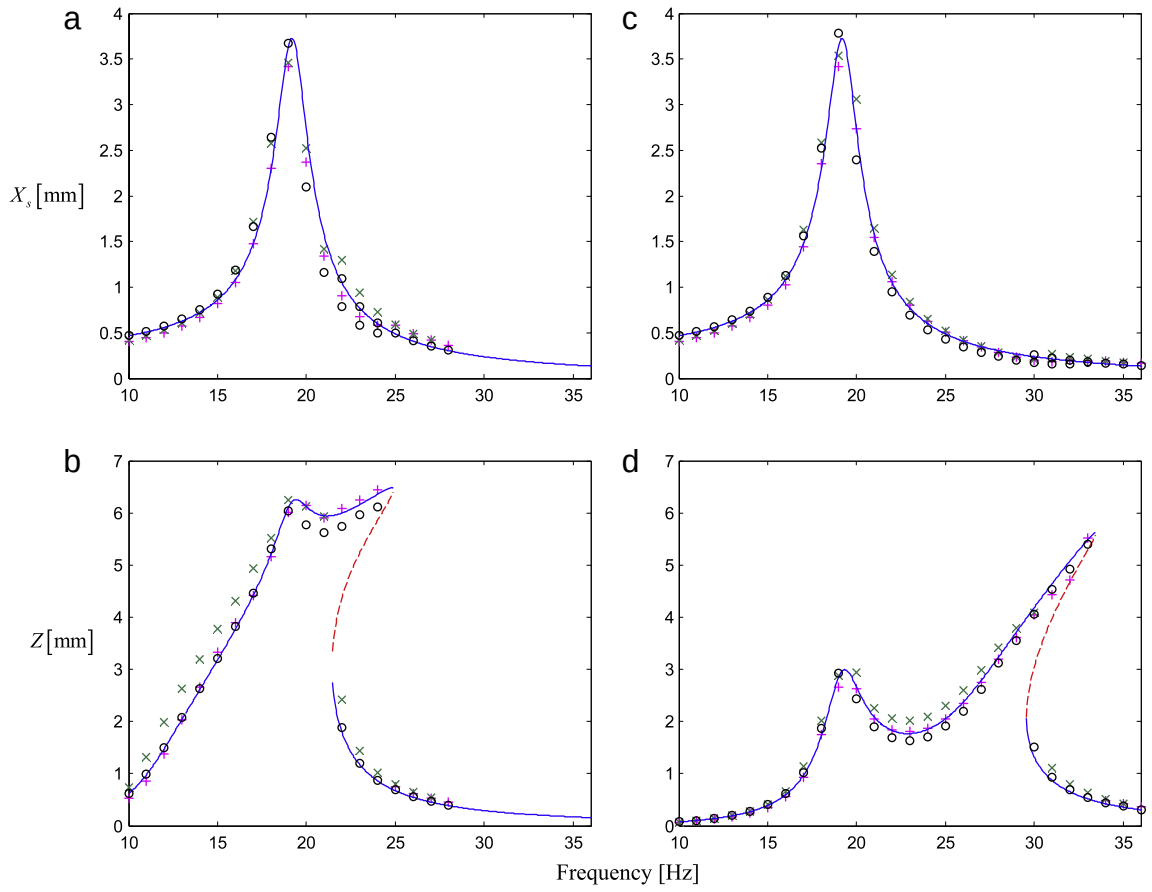

Fig. 6. Analytical, simulated and experimental results for a stepped-sine input to the shaker with a constant force amplitude. Wires with a low initial tension: (a) Absolute displacement of the support structure, (b) Relative displacement between the suspended mass and support structure. Wires with a high initial tension: (c) Absolute displacement of the support structure, (d) Relative displacement between the suspended mass and support structure. HBM solution: stable solution (blue solid line), unstable solution (red dashed line). Numerical solution by integrating Eqs. (4a) and (4b) (black '○'). Experiment: increasing frequency (magenta '+'), decreasing frequency (green '×').

were also calculated by solving the equations of motion (Eqs. (4a) and (4b)) directly by numerical integration and the results of the first harmonic are plotted, as circles, in Fig. 6(a)–(d) as well. For the parameters of the experimental rig, the second and higher harmonics were found to be negligible compared to the first harmonic; the small differences between the analytical and numerical results around the resonances are due to the fact that the assumption that $|\mu\ddot{y}| \ll |\ddot{y}_s|$ does not hold in these frequency regions. Examining Fig. 6(a)–(d) it can be seen that there is reasonably good agreement between the approximate HBM solution and the experimental results. Thus, the analytical model qualitatively captures the behaviour of the system.

3. Interaction of the responses at the resonance frequencies

The model developed in the previous section is used here to qualitatively investigate the effects of the system parameters ω_0 and γ on the FRC of the relative displacement W, and in particular the interaction of the two resonances in a two dof system — one of them being linear and the other being nonlinear. For a two dof linear system, i.e. $\gamma = 0$, the interaction of the two resonances is well-known, and for convenience it is illustrated in the animation of movie 3, which shows the effect of decreasing the non-dimensional resonance frequency ω_0 of the oscillator when passing through the resonance frequency of the support structure, which is equal to unity in non-dimensional form. The damping parameters used for the simulations are $\zeta_s = 0.046$, $\zeta = 0.026$, while ω_0 decreases linearly from 1.5 to 0.05.

If the nonlinearity increases, then the interaction between the two resonances becomes stronger, in the sense that it changes the FRC shape completely, resulting in closed detached curves which can lie outside or inside the main FRC. This is illustrated in Fig. 7 (a)–(f) and in the animation of movie 4, where the nonlinear term has been set to $\gamma = 2 \times 10^{-3}$. Logarithmic scales for the displacement amplitude have been used so that the behaviour for different values of ω_0 can be clearly seen. In Fig. 7(a)–(b), the resonance frequency of the shaker system is lower than the resonance frequency of the attached system, which was the case in the practical situation discussed earlier. The resonance frequency of the attached system is then further gradually decreased and its effects are illustrated in Fig. 7(c)–(e); finally in Fig. 7(f), the resonance frequency of the attached system is one tenth of that of the shaker. Depending of the values of the system parameters, if ω_0 is decreased further then a detached curve outside the main curve may form as shown in movie 5, where the damping of the linear system has been increased to $\zeta_s = 0.06$.

The effect of increasing the nonlinearity, for fixed value of the primary resonance of the Duffing oscillator, is illustrated in Fig. 8 (a)–(f) and in the animation of movie 6, where the nonlinear term has been increased from $\gamma = 10^{-4}$ to $\gamma = 2 \times 10^{-3}$ in a logarithmic fashion, the primary resonance has been set to $\omega_0 = 0.6$ and $\zeta_s = 0.046$, $\zeta = 0.026$. It can be observed that, for very small values of γ, i.e. $\gamma < 10^{-5}$, the nonlinearity is negligible and the system response is single-valued. For higher values of γ, a closed detached resonance curve appears above the main FRC, with stable and unstable parts. As γ is further increased, this detached resonance curve approaches the main FRC (Fig. 8(a) and (b)). A further

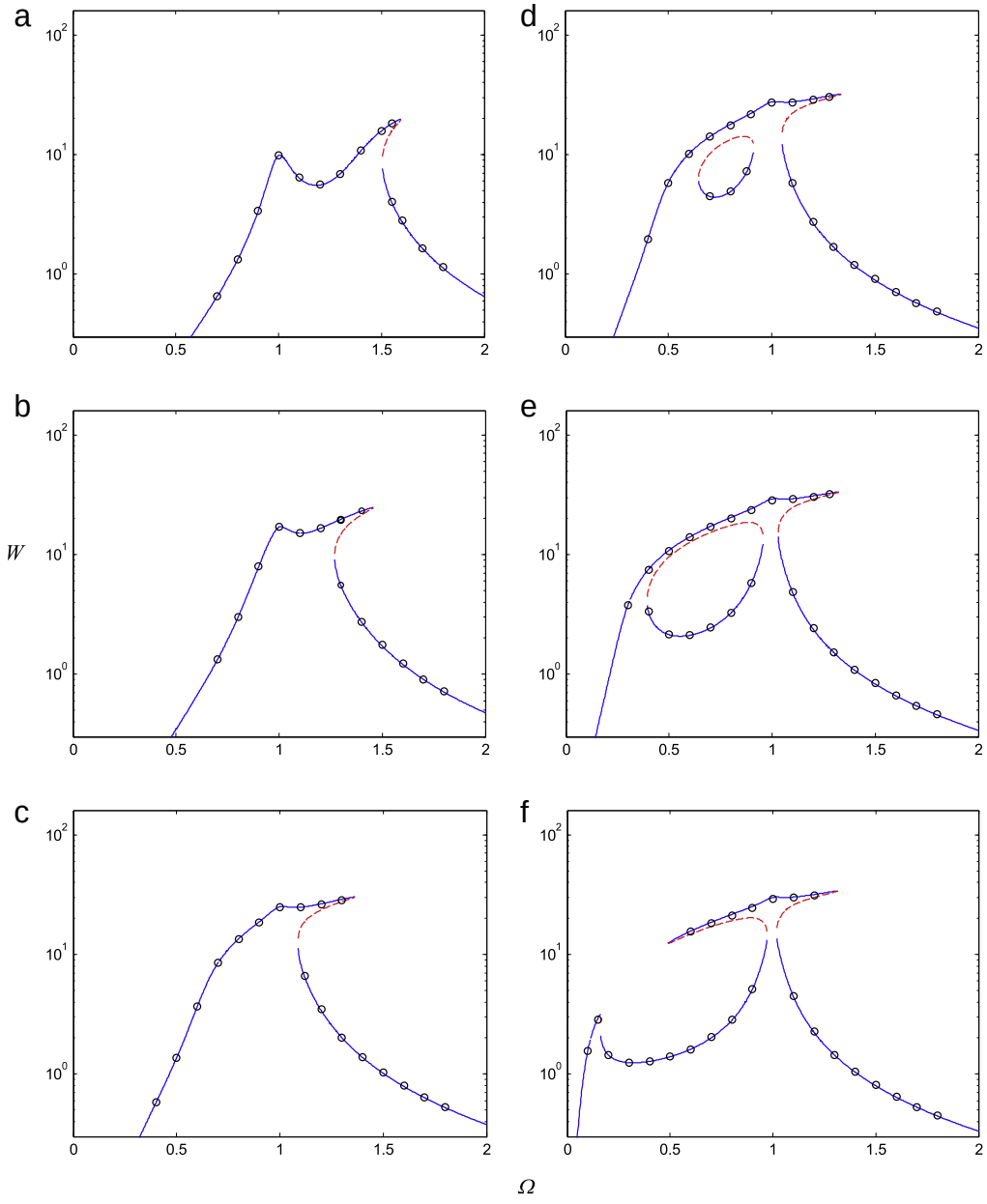

Fig. 7. FRCs of the normalised relative displacement W as a function of the normalised frequency, Ω, for $\gamma = 2 \times 10^{-3}$, $\zeta_s = 0.046$, $\zeta = 0.026$ and for different values of the normalised primary resonance of the oscillator: (a) $\omega_0 = 1.4$, (b) $\omega_0 = 1.1$, (c) $\omega_0 = 0.7$, (d) $\omega_0 = 0.5$, (e) $\omega_0 = 0.3$, (f) $\omega_0 = 0.1$. Stable solution (blue solid line), unstable solution (red dashed line). Numerical solution by integrating Eqs. (4a) and (4b) for $\mu = 0.001$ (black '○').

increase in γ causes the detached curve to join the main curve first at low frequencies (Fig. 8(c)) and then at $\Omega \sim 1$ to form another closed detached curve inside the main one (Fig. 8(d)) — the "bubble". The region of the frequency which the "bubble" covers becomes smaller as γ increases (Fig. 8(e)). The "bubble" disappears (Fig. 8(f)) for values of γ greater than approximately 1.5×10^{-3}. Depending of the values of the system parameters, the detached curve may also join the main curve first at $\Omega \sim 1$ and then at lower frequencies, as shown in the animation of movie 7, where the damping of the linear system has been decreased to $\zeta_s = 0.03$.

Note that in Figs. 7 and 8(a)–(f) unstable parts of the FRCs are indicated by dashed lines by applying the conditions for instability given by (8a, b). In addition, by numerical integration of the equations of motion, Eqs. (4a) and (4b), with the mass ratio fixed to $\mu = 0.001$ to satisfy the assumption $|\mu\ddot{y}| \ll |\ddot{y}_s|$, it is verified that the response of the system is periodic at the frequency of excitation, and higher harmonics are negligible. In Figs. 7(a)–(f) and 8(a)–(f), numerical solutions are also shown as circles as validation of the analytical results.

As noted above, the appearance of detached resonance curves inside or outside the main continuous one depends vitally on the values of the system parameters — damping in particular. A detailed analysis of the influence of damping on the shape of the FRCs has been performed by the authors and presented in [14].

4. An explanation for the shape of the FRC

The appearance of detached curves that lie outside or inside the main resonance curve implies the coexistence of steady-state responses with considerably different amplitudes. Their occurrence is dependent on the initial conditions.

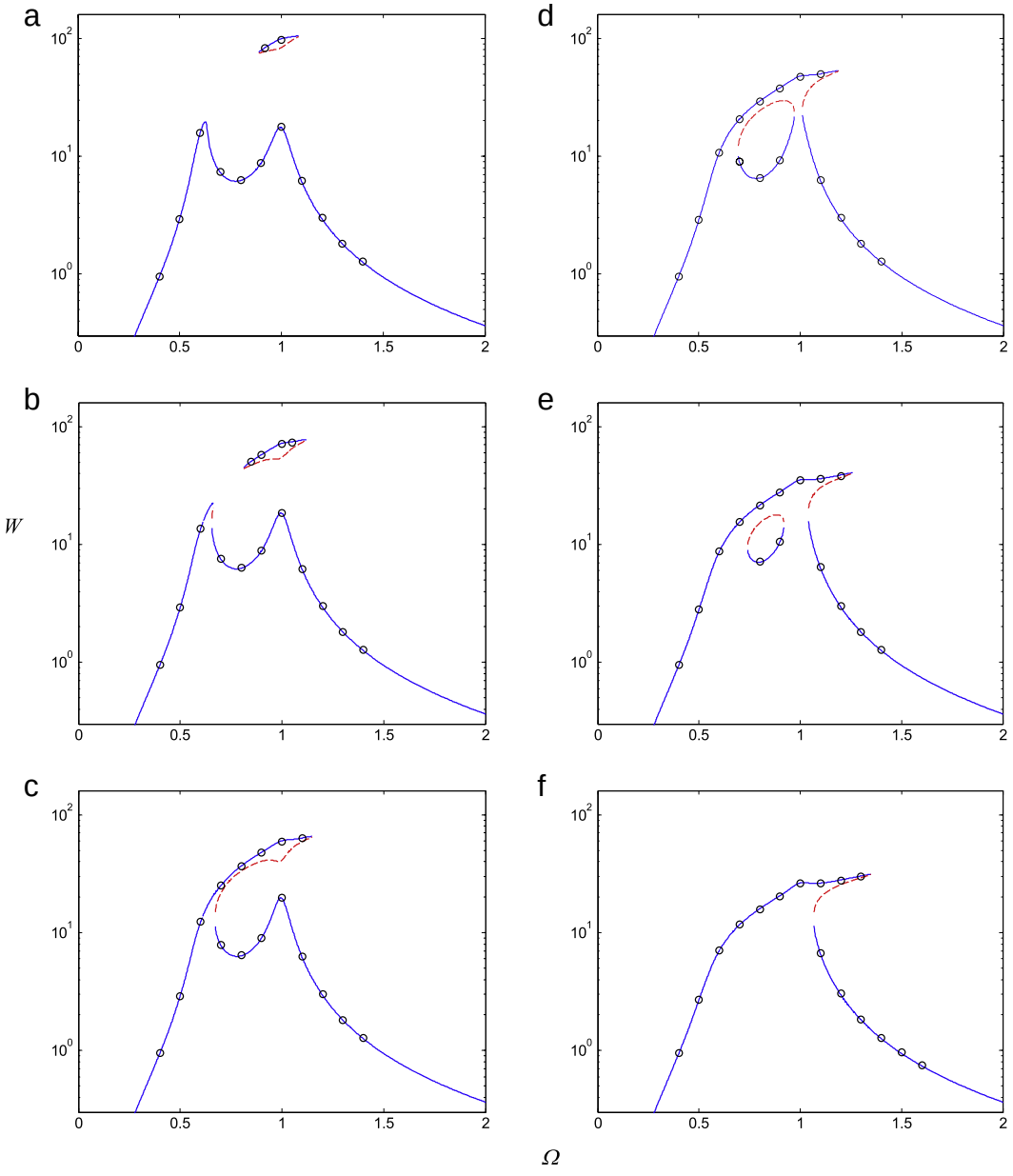

Fig. 8. FRCs of the normalised relative displacement W as a function of the normalised frequency Ω for $\omega_0 = 0.6$, $\zeta_s = 0.046$, $\zeta = 0.026$ and for different values of the nonlinear parameter: (a) $\gamma = 10^{-4}$; (b) $\gamma = 2 \times 10^{-4}$; (c) $\gamma = 3 \times 10^{-4}$; (d) $\gamma = 5 \times 10^{-4}$; (e) $\gamma = 1 \times 10^{-3}$; (f) $\gamma = 2 \times 10^{-3}$. Stable solution (blue solid line), unstable solution (red dashed line). Numerical solution by integrating Eqs. (4a) and (4b) for $\mu = 0.001$ (black 'o').

To further investigate the shape of the FRC and, in particular, the formation of the "bubble" it can be observed that the attached system is effectively driven by the shaker, such that the attached system has a negligible effect on the shaker at most frequencies. Accordingly, the attached system can be considered as a base-excited system in which the magnitude of the excitation is a function of frequency. The displacement of such a base excited system is described by Eq. (7a) and is shown in Fig. 9(a) (the green dashed line will be discussed later). A family of curves for a base-excited system with constant amplitude of excitation is shown in Fig. 9(b): the curves are labelled i–vi and correspond to the amplitudes of excitation shown in Fig. 9(a), with the corresponding labels. Also overlaid in Fig. 9(b) is the FRC of Fig. 8(e) (the graphs have linear scales for clarity). It can be seen that the family of curves is coincident with this curve at the frequencies marked with magenta diamonds. It is evident from this graph that the FRC of the relative displacement and the "bubble", in particular, is formed from the multiple solutions at the specific amplitudes of excitation and corresponding frequencies in the family of curves.

It is possible to take this analysis one step further by noting that the frequencies at which a jump-up in the response occurs is the same in the base-excited systems as well as the two dof system. However, in the two dof system, there are three jump-up frequencies; two of these occur in the "bubble" — one at each end, and the other occurs in the main FRC. A general expression for the amplitude, Y_u at the jump-up frequency Ω_u for a base-excited Duffing oscillator is given in [15], which can be rewritten in terms of the variables used in this paper as

$$Y_u^2 = \frac{8}{81\Omega_u^4\gamma}\left(\left(\Omega_u^2 - \omega_0^2\right)^3 + 36\zeta^2\Omega_u^2\left(\Omega_u^2 - \omega_0^2\right) + \left(\left(\Omega_u^2 - \omega_0^2\right)^2 - 12\zeta^2\Omega_u^2\right)^{\frac{3}{2}}\right). \tag{9}$$

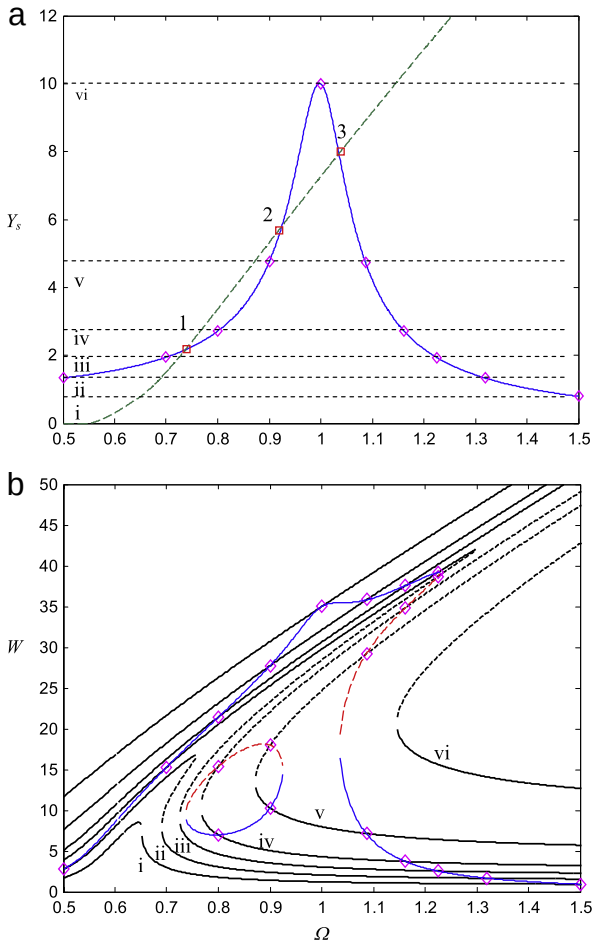

Fig. 9. Equivalence to a base-excited system. (a) Normalised absolute response of the support structure of the two dof system (blue solid curve), where dashed black lines i–vi indicate the input displacement amplitudes used to generate the family of curves i–vi in (b) and magenta '◇' indicate their intersections to the solid blue curve; the amplitude of Y_s at the jump-up frequency of the equivalent base-excited system (green dashed curve), where red '□' indicate the jump-up frequencies for the FRC of Fig. 8(e) overlaid in (b). (b) The family of curves for the amplitude response of the equivalent base-excited system for the different levels of input displacement i–iv in (a) (black solid and dashed curves), where magenta '◇' indicates the amplitudes of the response at the frequencies corresponding to the '◇' in (a); FRC of the normalised relative displacement W in Fig. 8(e) (blue solid and red dashed curves).

This is plotted as a green dashed line in Fig. 9(a). Its intersection with the graph for Y_s gives the frequencies at which the response jumps up; the intersections marked 1 and 2 correspond to the frequencies at the left and right-hand of the "bubble" respectively. The intersection marked 3 corresponds to the jump-up frequency in the main FRC.

5. Conclusions

In this paper, an investigation into the dynamics of a nonlinear system attached to a shaker which was driven harmonically, has been presented. The mass of the nonlinear system was much less than the support structure connecting it to the shaker, consequently the nonlinear system had a negligible effect on the response of the shaker for most frequencies. The nonlinearity of the attached system was due to the particular geometrical configuration of the springs. The system was modelled using the harmonic balance method to determine the primary frequency response equations and the stability conditions which define the stable and unstable steady-state solutions. The system of equations was decoupled and solved in closed form. Good agreement was found between the experimental results and the analytical and numerical solutions.

The effect of such nonlinearity was then further investigated through simulations and it was found that the frequency response curves for the two dof system can have unusual shapes. In particular, closed detached resonance curves can appear. They can lie outside or inside the main resonance curve and have stable and unstable parts. The latter has a shape of a "bubble" and the reason for this phenomenon was investigated using a family of base-excited Duffing oscillators with different excitation levels.

Acknowledgements

The first author would like to acknowledge the financial support of Regione Calabria (FSE-POR CALABRIA 2000-2006 Mis.3.7 Az.3.7B Cap.3421107) for covering travel and accommodation expenses at the Institute of Sound and Vibration Research (UK). Professors Brennan and Kovacic would like to acknowledge the support received from the Royal Society, UK, International Joint Project' 'Using nonlinearity to improve the performance of vibrating systems'.

The authors would also like to acknowledge the helpful discussions with Dr Dane Quinn from the University of Akron, concerning some of the features of the frequency response curves.

Appendix. Supplementary data

Supplementary data associated with this article can be found, in the online version, at doi:10.1016/j.physd.2010.01.006.

References

[1] J. Shaw, S.W. Shaw, A.G. Haddow, On the response of the non-linear vibration absorber, Internat. J. Non-Linear Mech. 24 (1989) 281–293.
[2] S.J. Zhu, S.J. Zhu, Y.F. Zheng, Y.M. Fu, Analysis of non-linear dynamics of a two-degree-of-freedom vibration system with non-linear damping and non-linear spring, J. Sound Vibration 271 (2004) 15–24.
[3] O.V. Gendelman, E. Gourdon, C.H. Lamarque, Quasiperiodic energy pumping in coupled oscillators under periodic forcing, J. Sound Vibration 294 (2006) 651–662.
[4] E. Gourdon, N.A. Alexander, C.A. Taylor, C.H. Lamarque, S. Pernot, Nonlinear energy pumping under transient forcing with strongly nonlinear coupling: Theoretical and experimental results, J. Sound Vibration 300 (2007) 522–551.
[5] O.V. Gendelman, Y. Starosvetsky, M. Feldman, Attractors of harmonically forced linear oscillator with attached nonlinear energy sink I: Description of response regimes, Nonlinear Dyn. 51 (2008) 31–46.
[6] Y. Starosvetsky, O.V. Gendelman, Attractors of harmonically forced linear oscillator with attached nonlinear energy sink. II: Optimization of a nonlinear vibration absorber, Nonlinear Dyn. 51 (2008) 47–57.
[7] Y. Starosvetsky, O.V. Gendelman, Response regimes of linear oscillator coupled to nonlinear energy sink with harmonic forcing and frequency detuning, J. Sound Vibration 315 (2008) 746–765.
[8] A. Jiang Xiaoai, M. McFarland, L.A. Bergman, A.F. Vakakis, Steady state passive nonlinear energy pumping in coupled oscillators: Theoretical and experimental results, Nonlinear Dyn. 33 (2003) 87–102.
[9] Y. Starosvetsky, O.V. Gendelman, Vibration absorption in systems with a nonlinear energy sink: Nonlinear damping, J Sound Vibration (2009), in press (doi:10.1016/j.jsv.2009.02.052).
[10] N.A. Alexander, F. Schilder, Exploring the performance of a nonlinear tuned mass damper, J. Sound Vibration 319 (2009) 445–462.
[11] M.N. Hamdan, T.D. Burton, On the steady state response and stability of non-linear oscillators using harmonic balance, J. Sound Vibration 166 (1993) 255–266.
[12] A. Hassan, On the local stability analysis of the approximate harmonic balance solutions, Nonlinear Dyn. 10 (1996) 105–133.
[13] M.J. Brennan, I. Kovacic, A. Carrella, T.P. Waters, On the jump-up and jump-down frequencies of the Duffing oscillator, J. Sound Vibration 318 (2008) 1250–1261.
[14] G. Gatti, I. Kovacic, M.J. Brennan, On the response of a harmonically excited two degree-of-freedom system consisting of a linear and a non-linear quasi-zero stiffness oscillator, J. Sound Vibration (November) (2009) (in press).
[15] Z. Milovanovic, I. Kovacic, I.M.J. Brennan, On the displacement transmissibility of a base excited viscously damped non-linear vibration isolator. ASME J. Vibr. Acoust. (2009), in press (doi:10.1115/1.3147140).